SAR Levels in Microwave Breast Imaging: 3-D Safety Assessment with Plane-Wave Illumination

Adam Santorelli, Michael Vander Schueren, Milica Popović

Department of Electrical and Computer Engineering, McGill University
Montreal, Canada
{adam.santorelli, michael.vanderschueren}@mail.mcgill.ca
milica.popovich@mcgill.ca

***Abstract* — In this work, we present results of simulation analysis to assess the safety of the microwave-based breast cancer detection techniques. In our numerical experiments, a detailed, three-dimensional anatomical model, derived from magnetic resonance images, has been exposed to plane waves from different angles and at varying frequencies. These simulations result in profiles of specific absorption rate (SAR), a quantity that is used to measure the compliance with safety standards. Our analysis implies that the power levels needed for the functioning of microwave breast cancer detection systems remains safe in terms of acceptable SAR levels.**

***Index Terms* — cancer detection, radiation safety, microwave imaging, numerical simulations.**

I. Introduction

Breast cancer is the most commonly diagnosed non-melanoma skin cancer amongst women worldwide. In Canada alone, it is estimated that over 23 000 women will be diagnosed with cancer in 2011. Early detection is pivotal for the successful treatment of the disease. The current gold standard for early screening is mammography, however due to the requirements of a biopsy for confirmation, the use of ionizing radiation, as well as issues with the occurrence of false positives, there continues to be a search for complimentary imaging modalities [1]. Microwave imaging has shown promise as a possible supplementary to mammography as an early-stage detection technique [2]. Studies show that the malign tissue in the breast can be detected with microwave illumination, due to the intrinsic electrical differences between the healthy and tumourous tissue at these frequencies. However, when exposing human tissues to microwaves, the consequent heating may result in tissue damage [3]. Hence, one must assess the exposure levels and ensure that they are within the safety limits determined by the relevant authorities.

We report the results from conducting a finite-difference time-domain (FDTD) analysis of the energy deposited within the human breast from exposure to an incident plane wave over the 0.4 - 9 GHz range by computing the local SAR values. Previously reported safety studies offer excellent guidance, however, they involve either two-dimensional (2-D) models or tissue properties reported prior to the extensive tissue characterization reported in [5]. In our simulations the breast is modeled as an anatomically realistic 3-D numerical phantom based on data from MRI-images. This heterogeneous breast model has tissue properties which are based on the data obtained from excised breast tissues [5].

II. Background

Microwave imaging for breast cancer detection is based on the inherent difference between the dielectric properties of healthy and malignant tissues of the breast. These differences, while being the very foundation of the microwave breast cancer detection methodology, are also the cause of non-uniform scattering and absorption of the microwave energy throughout the complex breast tissue structure.

At frequencies greater than 100 kHz the primary cause of damage to human tissue from EM exposure is due to heating effects and not electro-stimulation [3]. Commonly, the established safety standards consider the SAR as the appropriate measure for the energy deposited in the human tissue [6].

Table I includes data relevant to the SAR safety limits for different settings. Since the aim of microwave imaging for breast cancer screening is to create an imaging device which is readily available to the public, it is necessary to ensure that the standards for an uncontrolled environment are met. Furthermore, this imaging modality involves the localized exposure of the breast to EM fields. It is therefore paramount to ensure that peak local SAR values adhere to the standards set for the maximal peak averaged over a small amount of mass as opposed to the whole body (WB) average [6]. Peak local SAR values, as seen in Table I, can be averaged over 1 gram (1G) or 10 grams (10G) of tissue.

Previously, work done by Zastrow et al. concluded that the amount of energy deposited within the breast from the application of microwave imaging modalities is in compliance with current safety limits [4]. However, their model did not use the recently reported tissue data (Lazebnik et al.) obtained over the microwave range and compiled from the excised tissue in reduction and cancer surgeries [5], but instead made use of the data in [7]. The data compiled in [5] has been used in the development of recent numerical 3-D breast models such as those in [8]-[9]. This paper employs the

numerical breast model developed in [9] in order to present a safety assessment that is based on this new, more accurate, data.

TABLE I
SAR EXPOSURE LIMITS

	Controlled Environment [W/kg]	Uncontrolled Environment [W/kg]
SAR_{WB}	8	1.6
SAR_{1G}	20	4
SAR_{10G}	0.4	0.08

III. MODELS AND METHODS

All modeling and simulations are done in the commercial FDTD solver software SEMCAD-X [10]. The development of the 3-D numerical breast model in [9] has been tailored to facilitate its efficient use in commercial software such as SEMCAD-X.

The geometry of the breast model is derived from MRI images, differentiating tissues of the model by the varying levels of pixel intensities. As described in [9], this pixel intensity is then mapped to corresponding permittivity and conductivity values based on the data in [5]. This process ensures that the numerical breast phantom retains the inherent heterogeneity of the human breast while optimizing the computational resources required for FDTD simulations [9].

The complete simulation environment consists of the breast model, a skin layer, the chest wall, and a matching medium. The skin layer is a 1.5-mm thick layer surrounding the breast, whereas the chest wall consists of the 1.5-mm skin layer, a 3-mm thick fat layer, and a 5-mm muscle layer. A tumour cluster 4-mm in diameter is embedded within the breast. The conductivity of tumour cells is higher than surrounding adipose tissue, thus, we include the tumour in the model to investigate the occurrence of a local peak. The complete simulation environment is embedded in a canola oil matching medium in order to reduce reflections at the matching medium-skin interface [11].

These tissues, including those of the interior of the breast, are modeled in SEMCAD-X as dispersive materials which behave in agreement with the single-pole Debye model listed below in (1), where $\varepsilon(\omega)$ is the complex permittivity, ε_o is the permittivity of free space, ε_∞ is the dielectric constant of the material at infinite frequency, ε_s is the static dielectric constant, σ_s is the static conductivity, τ is the pole relaxation constant, and ω is the angular frequency:

$$\boldsymbol{\varepsilon(\omega) = \varepsilon_o \left(\varepsilon_\infty + \frac{\sigma_s}{j\varepsilon_0\omega} + \frac{\varepsilon_s - \varepsilon_\infty}{1 + j\omega\tau}\right)} \quad (1)$$

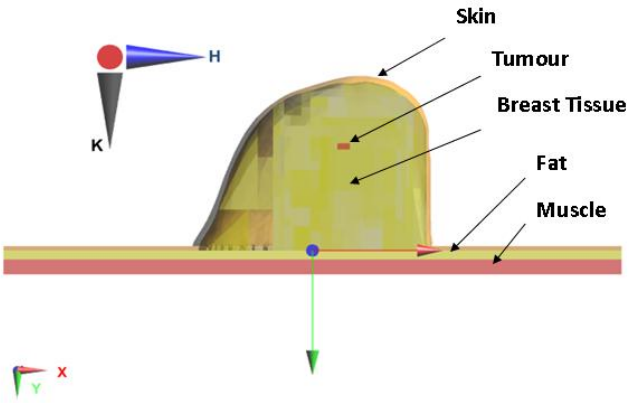

Fig. 1. Simulation environment, including the breast model and the chest wall. The picture demonstrates a cross-section perpendicular to the chest wall plane and located, roughly, in the middle of the breast model to show the tissues included in the model. For this particular case, the k-vector, indicating the propagation direction of the plane wave, is incident from the top of the breast model (in the opposite direction to the *y*-axis).

Table II lists the parameters implemented within SEMCAD-X to describe the Debye model for the skin layer, chest wall layer, tumour, and the matching medium. The properties of the interior breast tissue regions have been previously described in [9].

The safety assessment is carried out by exposing the breast model to an incident plane wave over a select number of frequencies over the 0.4 - 9 GHz range and calculating the local peak SAR values within each voxel and averaged over 10*g* of tissue. Select frequencies have been chosen to adhere to possible ISM bands reserved for medical imaging [12].

TABLE II
DEBYE PARAMETERS DESCRIBING DISPERSIVE MODEL

	Canola Oil	Skin	Fat	Muscle	Tumour
ε_s	2.51	39.8	4.71	54.9	55.1
ε_∞	2.28	15.9	3.12	21.7	6.75
σ_s [S/m]	0.008	0.831	0.050	0.886	0.790
τ [psec]	27.8	13.0	13.0	27.8	10.5

Two angles of incidence for the plane wave have been chosen (as depicted in Fig. 1). In the first case, the plane wave is incident laterally, to the breast side, and propagating in the *z*-direction. In the second case, the plane wave is propagating in the direction opposite to the *y*-axis, towards the chest wall; hence, we refer to this direction as "from the top". The input power for the plane wave has been selected to adhere to the maximum permissible incident energy as described in [3], akin to the decision made in [6]. This information is presented in Table III.

TABLE III
INCIDENT POWER SELECTION PER FREQUENCY

f [GHz]	P_{INC} [W/m^2]	f [GHz]	P_{INC} [W/m^2]
0.434	2.893	4	10.00
0.915	6.100	5	10.00
1.5	10.00	5.8	10.00
2	10.00	7	10.00
2.45	10.00	8	10.00
3	10.00	9	10.00

IV. RESULTS

The following section presents the data obtained from the FDTD simulations run within SEMCAD-X. We present and contrast the results from the unaveraged local peak SAR values and the peak SAR values averaged over 10-g of tissue for the *z*-directed and *y*-directed plane wave.

The peak unaveraged SAR values are representative of the worst-case scenario. These values are computed for the selected frequencies of interest and are presented in Fig. 2 for both incident plane waves. A first order least-squares fit is used to represent the data with r^2-values of 0.9013 and 0.7225 for the *z*-directed and *y*-directed plane wave respectively. This fit demonstrates that the relationship between the frequency of the incident plane wave and the amount of energy deposited in the breast can be well explained by a linear model. Particularly, as the frequency of the plane waves is increased we can expect the heating of the tissue to become more pronounced, as evidenced by the higher peak SAR values.

The data in Fig. 2 show that the maximum local peak SAR values, 24mW/kg and 17mW/kg for the laterally-incident and top-incident plane waves, respectively, adhere to the most stringent limits set in Table I.

A profile of SAR values within the breast for a cross-section in the model is shown in Fig. 3; these are peak, not averaged SAR values. We note that for the *z*-directed plane wave the peak SAR values occur at the skin-matching medium interface, as well as near the skin-chest wall interface. In the case for the *y*-directed plane wave, we observe that the peak SAR values appear within the muscle layer of the chest wall. Peak values also occur along the skin portion of the chest wall and in the skin near the nipple area.

The SAR values have also been averaged for 10-g tissue over the selected frequencies noted in Table III. As was done in Fig. 2, we attempt to demonstrate a relationship between the frequency of the plane wave and the resulting SAR values. Fig. 4 presents the measured values, denoted by markers, as well as a first-order least-squares model used to fit the data. Although the linear fit does not represent data well, we show it for completeness and make a note of the corresponding r^2-values of 0.1907 for the *z*-directed wave and 0.1823 for the *y*-directed wave. The maximum 10-g average SAR value, 1.7mW/kg and 1.5mW/kg for both the laterally-incident and top-incident plane waves, respectively, is well below the restrictive limits of Table III.

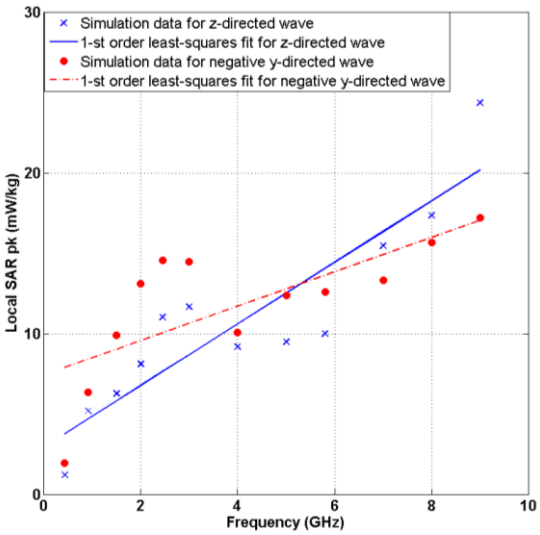

Fig. 2. The relationship between increasing frequency and the peak local SAR values recorded. The "○" and "x" markers correspond to the recordings from simulation for the *z*-directed and *y*-directed wave respectively. The solid and dashed lines correspond to the 1st order least-squares fit for each case.

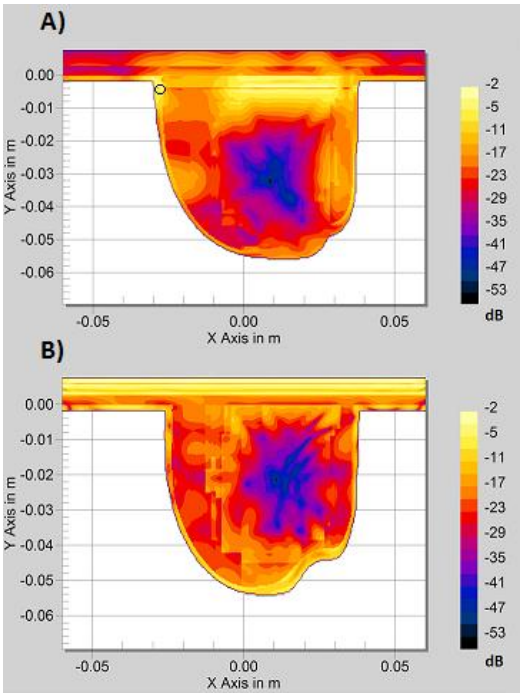

Fig. 3. The SAR values over the entire breast domain are shown in this 2-D image. The image is extracted from the 3-D data for a plane wave incident at 8GHz. Where (a), corresponds to the *z*-directed wave, and, (b), corresponds to the negative *y*-directed wave. The '○' marker corresponds to the max SAR value recorded.

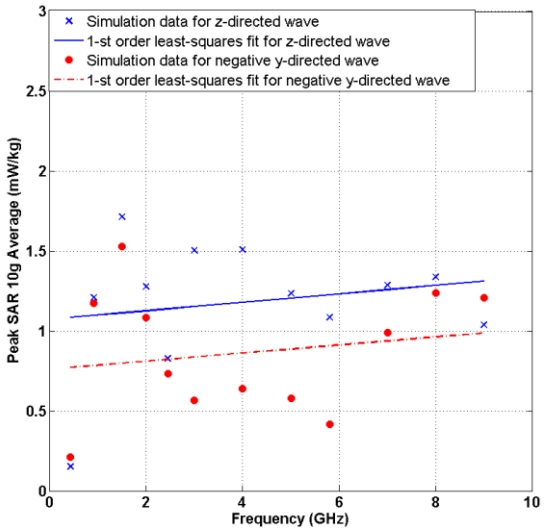

Fig. 4. The relationship between the recorded peak SAR 10-g average values and increasing frequency. The "○" and "x" markers correspond to the recordings from simulation for the *z*-directed and *y*-directed wave respectively. The solid and dashed lines correspond to the 1st order least-squares fit for each case.

We also notice that at very low frequencies, < 1GHz, the SAR values, for both the unaveraged and 10-g average, are lower than expected. This resonates with the fact that the exposure limits at these frequencies are much more stringent than at higher frequencies [4].

V. Conclusion

We have shown that, based on both the local peak and 10-g average SAR values, the amount of energy deposited within the breast in microwave imaging techniques falls well below the established maximum values, regardless of the angle of the incident plane wave, validating the safety of the technique. For both angles of incidence of the plane wave, the peak local SAR values occur in the skin; however, the location of this peak is dependent on the angle of incidence.

In this work we have assumed a plane wave to be the power source illuminating the breast. This corresponds to a worst-case scenario, where the entire breast region is being irradiated. In microwave imaging for breast cancer detection the power source used to illuminate the breast is predominantly a highly directional antenna. Future work involves determining whether the antenna pattern will affect the peak SAR values, as well as the locations of these peaks, and identifying the maximum amount of power the antenna can send before approaching the consequent maximum permissible SAR levels in the tissue.

Acknowledgement

The authors are grateful for the funding support by the Natural Sciences and Engineering Research Council of Canada (NSERC), le Fonds québécois de la recherche sur la nature et les technologies (FQRNT), and Partenariat de Recherche Orientée en Microélectronique, Photonique et Télécommunications (PROMPT).

References

[1] Canadian Cancer Society. (2010, August 17). What is breast cancer? [Online]. Available: http://www.cancer.ca/

[2] E.C. Fear, P.M. Meaney and M.A. Stuchly "Microwaves for breast cancer detection?" *IEEE Potentials*, pp.12-18, February/March 2003.

[3] Health Canada, "Limits of Human Exposure to Radiofrequency Electromagnetic Fields in the Frequency Range from 3 kHz to 300 GHz: Safety Code 6 ," Health Canada, 2009.

[4] E. Zastrow, S. K. Davis, and S. C. Hagness, (2007), "Safety assessment of breast cancer detection via ultrawideband microwave radar operating in pulsed-radiation mode," *Microwave and Optical Technology Letters*. doi: 10.1002/mop.22089

[5] M. Lazebnik, D. Popovic, L. McCartney, C. Watkins, M. Lindstrom, J. Harter, S. Sewall, T. Ogilvie, A. Magliocco, T. Breslin, W. Temple, D. Mew, J. Booske, M. Okoniewski, and S. Hagness, "A large-scale study of the ultrawideband microwave dielectric properties of normal, benign and malignant breast tissues obtained from cancer surgeries," *Phys. Med. Biol.*, Vol. 52, pp. 6093-6115, 2007.

[6] P. Bernardi, M. Cavagnaro, S. Pisa, E. Piuzzi, "Specific Absorption Rate and Temperature Elevation in a Subject Exposed in the Far-Field of Radio-Frequency Sources operating in the 10-900-Mhz Range," *IEEE Trans. Biomed. Eng.*, vol. 50, pp. 295–304, March 2003.

[7] M. Converse, E. J. Bond, B. D. van Veen, and S. C. Hagness, "A computational study of ultra-wideband versus narrowband microwave hyperthermia for breast cancer treatment," *IEEE Trans. Microw. Theory Tech.*, vol. 54, no. 5, pp. 2169–2180, 2006.

[8] E. Zastrow, S. Davis, M. Lazebnik, F. Kelcz, B. V. Veen, and S. Hagness, "Development of anatomically realistic numerical breast phantoms with accurate dielectric properties for modeling microwave interactions with the human breast," *IEEE Trans. Biomed. Eng.*, vol. 55, no. 12, pp. 2792–2800, Dec. 2008.

[9] G. Zhu, B. Oreshkin, E. Porter, M. Coates, M. Popović "Numerical Breast Models for Commercial FDTD Simulators", in *Proc. European Conference on Antennas and Propagation (Eu-CAP'09)*, Berlin, Germany, Mar. 2009.

[10] SPEAG, Schmid & Partner Engineering AG. (2011, May 3). [Online].Available: http://www.speag.com/

[11] J. Bourqui, M. Okoniewski, E. C. Fear, "Balanced Antipodal Vivaldi Antenna With Dielectric Director for Near-Field Microwave Imaging", *IEEE Trans. on Antennas and Prop.,* VOL. 58, NO. 7, July 2010.

[12] ITU-R (2001). *Article 5 of the Radio Regulations*. [Online] Available: http://users.ictp.it/~puboff/lectures/lns016/Vol16Annex.pdf